Tribology Letters (2022) 70:114
https://doi.org/10.1007/s11249-022-01655-7

ORIGINAL PAPER

Starvation and Re-lubrication in Oscillating Bearings: Influence of Grease Parameters

Sebastian Wandel[1] · Norbert Bader[1] · Jakob Glodowski[1] · Bela Lehnhardt[1] · Johan Leckner[2,3] · Fabian Schwack[4] · Gerhard Poll[1]

Received: 10 July 2022 / Accepted: 12 September 2022 / Published online: 26 September 2022

Abstract

A common application for grease-lubricated oscillating rolling element bearings is, e.g., rotor blade bearings in wind turbines. These bearings mainly operate under conditions that are prone to starvation. If the grease is unable to provide enough inlet lubricant supply for the contact between rolling element and bearing raceway, wear in the form of False Brinelling and thus premature bearing failure is possible. Bearing experiments with different lithium complex model greases, which differ mainly in their base oil viscosity and oil separation rate, were carried out to show the influence of the grease parameters on wear initiation. The results show that the ability of the grease to release a high amount of base oil with high mobility into the track of the rolling element is a crucial mechanism to prevent wear, especially at small oscillation angles. For oscillation angles larger than a critical angle, a secondary replenishment mechanism may prevent early wear initiation. The experimental results are used to validate a starvation model proposed in earlier work (Wandel et al. in Tribol Int 165:107276, 2022).

Keywords Oscillating bearings · False brinelling · Starvation · Re-lubrication

Abbreviations

f	Oscillation frequency
f_c	Overrolling frequency
e	Amplitude ratio
e_{IR}	Amplitude ratio on the inner ring
θ	Oscillating angle
θ_{SW}	Starvation driven wear angle
θ_c	Critical oscillation angle
θ_{crit}	Critical oscillation angle according to Harris
θ_{dith}	Dither angle according to Harris
S_N	Starvation number
x	Traveled distance of contact ellipse
O_{SR}	Oil separation rate
x_{SW}	Traveled distance of contact ellipse corresponding to θ_{SW}
x_c	Critical traveled distance of contact ellipse
b	Short Hertz'ian half axis
b_{IR}	Short Hertz'ian half axis on the inner ring
a	Long Hertz'ian half axis
a_{IR}	Long Hertz'ian half axis on the inner ring
t_r	Replenishment time
t_c	Time between overrollings

Norbert Bader, Jakob Glodowski, Bela Lehnhardt, Johan Leckner, Fabian Schwack and Gerhard Poll contributed equally to this work.

✉ Sebastian Wandel
wandel@imkt.uni-hannover.de

Norbert Bader
bader@imkt.uni-hannover.de

Jakob Glodowski
jg.glodowski@web.de

Bela Lehnhardt
bela.lehnhardt@googlemail.com

Johan Leckner
johan.leckner@axelch.com

Fabian Schwack
Fabian.Schwack@gmx.de

Gerhard Poll
poll@imkt.uni-hannover.de

[1] Institute of Machine Design and Tribology, Leibniz University Hannover, An der Universitaet 1, 30173 Garbsen, Niedersachen, Germany

[2] Department of Machine Design, KTH Royal Institute of Technology, 10044 Stockholm, Sweden

[3] AXEL Christiernsson International AB, 44941 Nol, Sweden

[4] 8000 Aarhus, Denmark

σ_s Surface tension
η_0 Dynamic base oil viscosity

1 Introduction

Oscillating rolling element bearings play an important role in many industries. Whether in robotic arms or as rotor blade bearings in wind turbines, the bearing is a critical component for the function of the respective application [1, 2]. In earlier work, it was shown that operation with very small oscillation angles (vibration) can lead to standstill marks [3]. These standstill marks are characterized by the fact that the contact area is not fully exposed to fresh lubricant during an oscillation and the contact area can no longer be supplied with fresh lubricant. After an incubation phase, wear- and surface-induced cracking can be the result [4, 5]. When the oscillation angles are large enough so that the contact area opens up during an oscillation, the possibility of track replenishment through base oil reflow is given [6–12]. Nevertheless, these conditions can be prone to starvation and early wear commonly referred to as false brinelling, especially if the grease is unable to provide sufficient base oil with good lubricity [13, 14].

In general, it is assumed that smaller oscillation angles are more critical for wear initiation since no sufficient hydrodynamic lubricant film build up is possible [15].

In earlier work [16], we have shown that small oscillation angles are not necessarily more critical in terms of early wear initiation. Up to a starvation driven wear angle θ_{SW}, the conditions get more critical. For the used bearing type, this angle was in the range of 15°–30°. For bigger angles, a secondary re-lubrication mechanism becomes active and the conditions are less critical. It is expected that this re-lubrication is due to redistribution of the grease on the rolling element by the cage. It was suggested by Harris that the conditions are critical to early wear initiation up to a critical angle ω_{crit} calculated according to [17].

However, in our previous work, we have shown that this critical angle also depends on the nature of the lubricant.

To be able to estimate whether an oscillating bearing encounters starvation-driven wear, a starvation number S_N was introduced, which depends on the operating conditions as well as the grease parameters, see equation 1. The starvation number was adapted based on the work of Damiens, Cann and Cen [18–20]. The higher the starvation number, the more likely early wear initiation is. This starvation number is based on results obtained with two fundamentally different greases. The objective of this paper is to validate the suggested starvation number in oscillating grease-lubricated rolling element bearings with additive-free model greases, which are similar in terms of their thickener structure but differ in terms of base oil content and base oil viscosity.

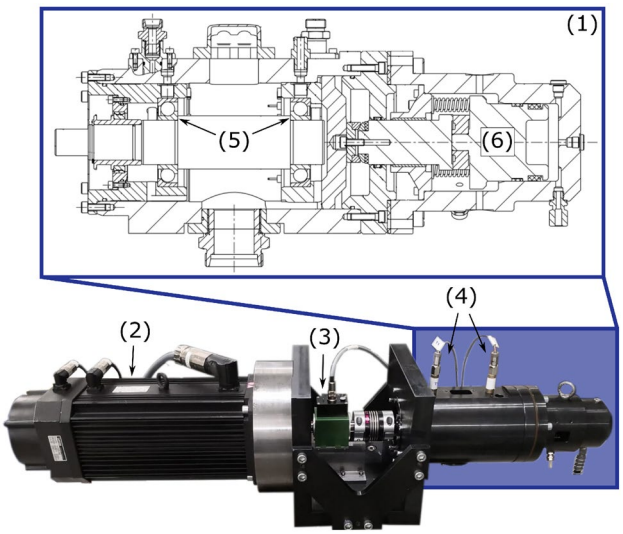

Fig. 1 Illustration of the test setup used [16]. (1) Test unit containing the type 7208 test bearings; (2) Asynchronous servo motor that applies a sinusoidal motion profile; (3) Torque transducer that measures the resistance to rotation of the test bearings; (4) PT100 temperature sensors; (5) Type 7208 test bearings; (6) Hydraulic load unit;

Based on the results, a critical starvation number SN_c will be suggested, which should not be exceeded in operation in order to avoid early wear initiation.

2 Experimental Setup

An oscillating bearing test rig, which was already used in [16], was used to carry out the experiments. Figure 1 shows the details of the experimental setup. The oscillating motion with adjustable frequency, amplitude and motion profile is given by a position-controlled asynchronous motor, which has already been part of previous publications [4, 21]. Between the motor and the test unit, a torque transducer with built-in incremental encoder allows the measurement of the angle synchronous torque. The test unit contains two unsealed angular contact ball bearings of type 7208 (FAG). The bearings are mounted in face-to-face arrangement and are axially loaded by a hydraulic load unit. A hydraulic control system ensures constant axial loading of the test bearings. During the experiments, the temperature of the bearings is monitored via PT100 elements on the outer ring.

A digital microscope is used to visually assess the bearing damage after the tests.

2.1 Experimental Conditions

Before a test run, each bearing is disassembled and all parts are cleaned for 5 min in an ultrasonic bath with benzine followed by a 5 min ultrasonic bath in isopropanol and 15 min

Table 1 Grease properties

Parameter	LiX4	LiX4+20%	LiX100	Industrial Grease 1	Industrial Grease 2
Thickener type	LiX	LiX	LiX	Li	Ca
Base oil type	93.7% PAO /6.3% ester	93.7% PAO /6.3% ester	93.7% PAO /6.3% ester	PAO	Mineral Oil
Base oil viscosity at 40 °C in cSt	19	19	1067	50	13
Density at 40 °C in 10^{-3} Kg/m^3	0,82	0,82	0,84	0,83[1]	0,83[1]
Base oil viscosity at 40 °C in Pas	0,0171	0,0171	0,9603	0,045	0,0117
Surface tension in 10^{-3} N/m	28.54	28.54	31.16	30[2]	30[2]
Oil separation rate O_{SR} in % (IP 121)	0.7	5.1	1.2	4.0	6.1
Pen60 1/2-scale in 10^{-1} mm	276	317	276	319	305
NLGI grade	2	1	2	1	0–1
x_{SW} in 10^{-3} m	3,75	3,75	3,75	3,75	7,5
x_c in 10^{-3} m	7,5	7,5	7,5	7,5	15

[1] Assumption for the density, as exact measurements are not available.

[2] Assumption for the surface tension, as exact measurement are not available

of drying in an oven at 80 °C. Afterward, the bearings are reassembled and mounted on the shaft before grease is filled into the bearing. This is done after the bearings have been mounted on the shaft to protect the grease from heat during assembly. Then, a syringe is used to fill 100 % of the free bearing volume with grease. This corresponds to 10 ml of grease per bearing. Further information on the model greases used can be found in Sect. 2.2. All experiments shown in this paper were performed with a constant axial load of 12.4 kN, resulting in a maximum contact pressure of approximately 2 GPa between rolling elements and raceways.

The bearings are rotated continuously at 10 rpm for 20 revolutions under applied axial load to ensure uniform grease distribution at the start of the test. The actual test run then starts, and the bearings are subjected to a sinusoidal oscillation for 4000 cycles. The varied test parameters are oscillation frequency and oscillation angle. The combinations of the oscillation frequencies and angles shown in Table 2 are used.

The amplitude ratio $e = x/2b$ is used to select the range of oscillation amplitudes. The angle that limits the oscillation frequency downward is the dither angle $e = 1$ [22]. For smaller angles, the contact area is not fully opened[1] during an oscillation and standstill marks may result. For larger angles, the critical angle that was suggested by Harris limits the oscillation angle upward. Larger angles lead to an overlap of the contact areas of adjacent rolling elements. For the operating conditions selected in this paper, overlapping occurs on the inner ring from an amplitude ratio of $e_{IR} = 32.5$ upward. A more detailed explanation of the operating conditions chosen for the experiments can be found in [16]. Explanations regarding the dither angle and the critical angle can be found in Harris et al. [22]. Experiments based on this definition were carried out by Maruyama et al. [15] and Schwack et al. [23].

2.2 Model Greases

The lithium complex model greases were produced in a laboratory reactor using a batch size of 8 kg. The manufacturing process followed a standardized procedure where the soap was made in approximately 40% of the total oil content. The first saponification reaction using 12-hydroxyoctadecanoic acid was performed at 90 °C with a hold time of 30 minutes. The temperature was subsequently raised to around 115 °C and then kept steady for two hours. At this point, the second saponification reaction using azelaic acid was performed. The grease was then kept steady at 115 °C for an additional half hour before the temperature was raised to the maximum temperature of 205 °C. The cooling was accomplished using 5 % portions of oil with a hold time of 15 minutes after each

Table 2 Parameter combinations

Parameter	Value	Unit
Axial load	12.4	kN
a_{IR}	1.6	10^{-3} m
b_{IR}	1.7	10^{-4} m
Frequency f	0.2, 1, 3, 5	Hz
Angle θ	2, 7, 15, 30, 45	°
Distance x	5, 17.5, 37.5, 75, 113	10^{-4} m

[1] We use the description "opened" to describe whether the contact patch moves relative to the starting position.

addition. The grease was finally passed through a colloidal mill after which it was deaerated for 1 hour. The base oil is a blend that consists of 6.3 % adipate ester and 93.7 % PAO, where the PAO is either a PAO4 (LiX4 grease) or a PAO100 (LiX100 grease). Most of the ester was used up front in the process to facilitate the saponification reactions. Only small amounts of ester were added in the end of the process to ensure identical oil composition. The LiX4 grease diluted with 20 % additional oil blend was mixed using a DAC-600 SpeedMixer until completely homogeneous and is called LiX4+20 hereafter. All three grease were passed through a 3-roller mill three times prior to testing to reset any possible structure that might have built up during storage. The grease properties can be found in Table 1. It includes the properties of the model greases that were examined in the course of this paper, as well as two industrial greases that were tested under the same conditions in the last paper [16].

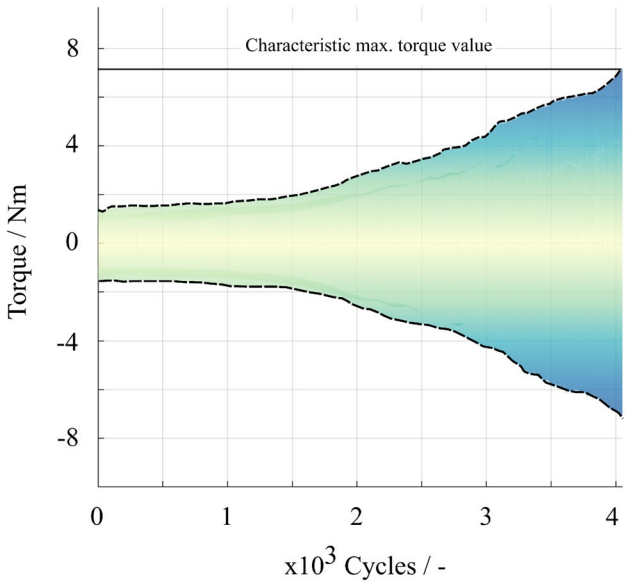

Fig. 2 Measured torque signal reduced by the moment of inertia of the moving components for a test at f= 3 Hz, Θ= 7°. The black dashed lines show the development of the maximum and minimum torque. The solid black line marks the maximum torque value that was reached during the test [16]

3 Results

The results section contains the analysis of the measured torque and builds a connection to the phenomenological observation of the damage on the bearing raceway. The results are aggregated and visualized in color maps and then compared to the previously suggested starvation number *SN*. The temperature change measured on the outer ring during the tests was negligibly small, regardless of the operating parameters, so it will not be discussed in more detail below.

3.1 Analysis of the Experimental Data

During the experiments, the angle synchronous torque is recorded and subsequently reduced by the moment of inertia of the moving components. Figure 2 shows the development of torque over the number of oscillating cycles for a test run at 3 Hz oscillation frequency and 7° oscillation angle. The black dashed lines in Fig. 2 show the course of the maximum and minimum torque during the test. A comparison of the results is made on the basis of the curves of the absolute maximum values of the torque per oscillation cycle.

Figure 3 shows all the results for the different operating parameters and the different model greases. The diagrams in the left column show the results for grease LiX4. The upper left diagram shows the results for the different oscillation angles at the lowest oscillation frequency of 0.2 Hz, the further down in the diagram, the higher the oscillation frequency up to 5 Hz. The same principle applies for the middle column with grease LiX4+20 and the right column with grease LiX100. The oscillating amplitudes are shown with different line styles. The abscissa shows the number of cycles, i.e., experimental time.

Comparing the diagrams at an oscillation frequency of 0.2 Hz, it is clear that the torque for LiX4 remains constant over the entire duration of the experiments and over the whole range of tested oscillation amplitudes. The representative raceway surface for these operating conditions can be seen in Fig. 4a. The raceway surface shows no signs of adhesive damage. The same applies to the LiX4+20 grease with increased base oil content, again no increase in torque as well as no damage on the raceway surface could be detected. In contrast, the torque for LiX100 increases sharply from the start for all angles except for 45°. At 2°, the sharp increase at the beginning up to 5.6 Nm is followed by a sharp drop down to a low level of about 1.2 Nm where it remains constant over the course of the experiment. Looking at the damage on the raceway surface in Fig. 4b, we can see that a part of the covered track shows corrosive damage. This initiation occurred at the beginning of the experiment during the sharp torque rise. The tests at 7°, 15° and 30° remain at a higher torque level, with the test at 7° showing a downward trend, while the tests a 15° and 30° show an upward trend. By far, the highest torque of 13 Nm is reached at an oscillation angle of 15°. The corresponding representative damage mark can be seen in Fig. 4c. As expected from the high torque values, the whole covered track shows severe damage consisting of black and red iron oxide and a spotty surface due to material spalls.

Taking a look at the experiments for LiX4 at 1 Hz oscillation frequency, it can be seen that the torque values for

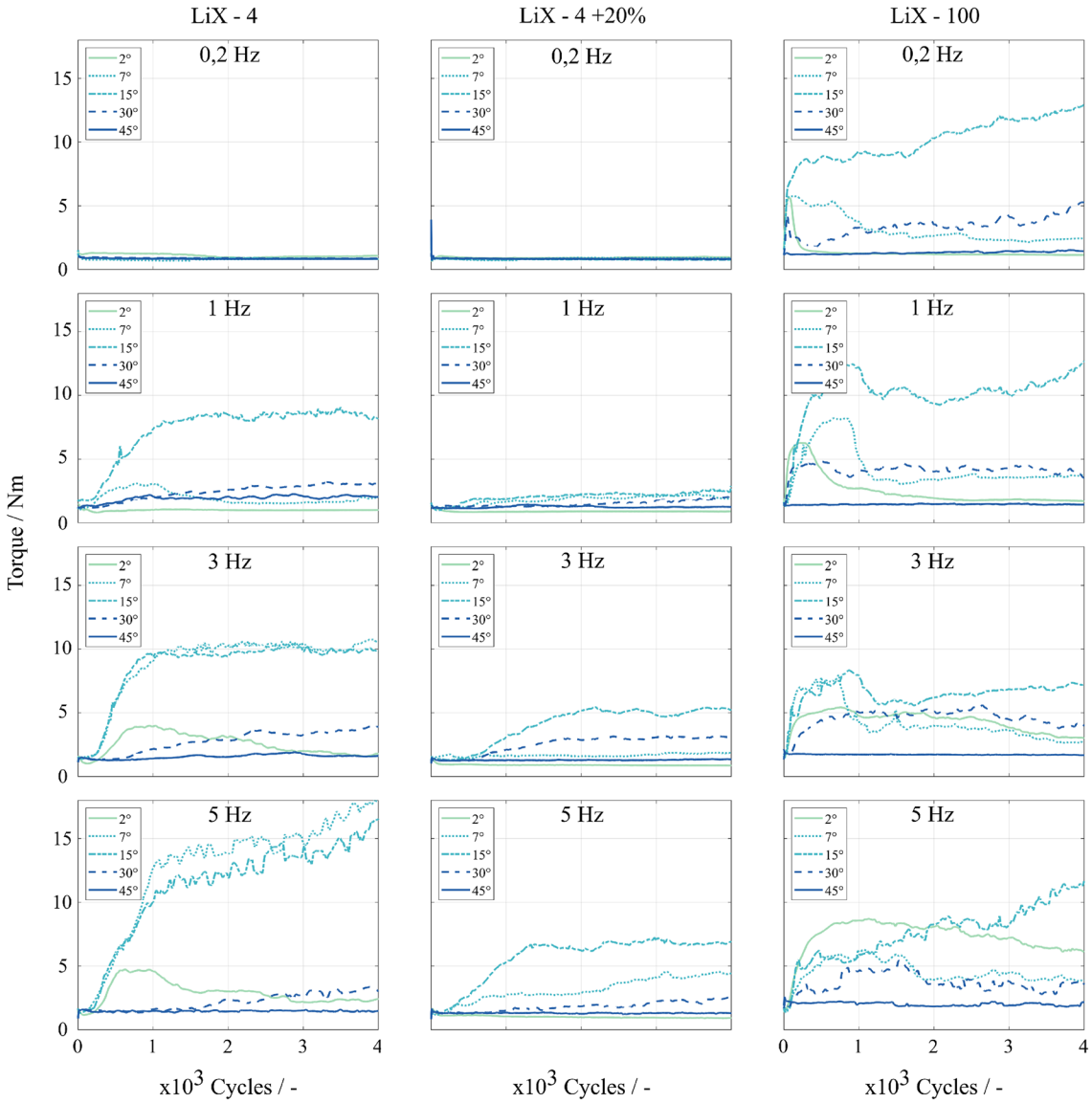

Fig. 3 Illustration of the progression of the maximum absolute torque value of every oscillation cycle for the tested parameter combinations and greases. The left column shows the results for grease LiX4, the middle column the results of LiX4 with 20 % extra base oil and the right column for LiX100. The upper row of diagrams shows the results for 0.2 Hz the bottom row for 5 Hz

the test at 2° stay at a constant low level. There is a slight increase in the torque for the tests at 7°, 30° and 45° and a sharp increase at 15° oscillation angle. Looking at the results for LiX4+20, the sharp increase in the torque at 15° was noticeably reduced. The torque curves of the other oscillation angles also show a smaller upward deflection. Looking at the test at 1 Hz for LiX100, it can be seen that the shape of the curves is very similar to those at 0.2 Hz. The only curve that constantly stays at a low level is at 45° oscillation angle. The second line of raceway images in Fig. 4 shows the damage marks for the tests with the different greases at 1 Hz and 15°. The comparison shows that for grease LiX4 (d)) and LiX100 (f)), the whole track covered by the contact area is severely damaged. A representative mark for the LiX4+20 grease (e)) with added base oil also shows the beginning of severe damage to parts of the covered surface, but in comparison with the other greases, the damage is less severe.

If the frequency is further increased to 3 Hz, there are two curves for the LiX4 grease, at 7° and at 15° oscillation angle, that show a sharp increase in torque up to about 10 Nm. The test at 2° also shows an upward deflection in contrast to the tests at 0.2 Hz and 1 Hz, but recovers to a low level in the course of the test. In this case, the representative damage mark in Fig. 4g shows a partially damaged raceway surface. For the grease LiX4+20, these operating conditions are not critical and no damage occurs, see Fig. 4h. Looking at the

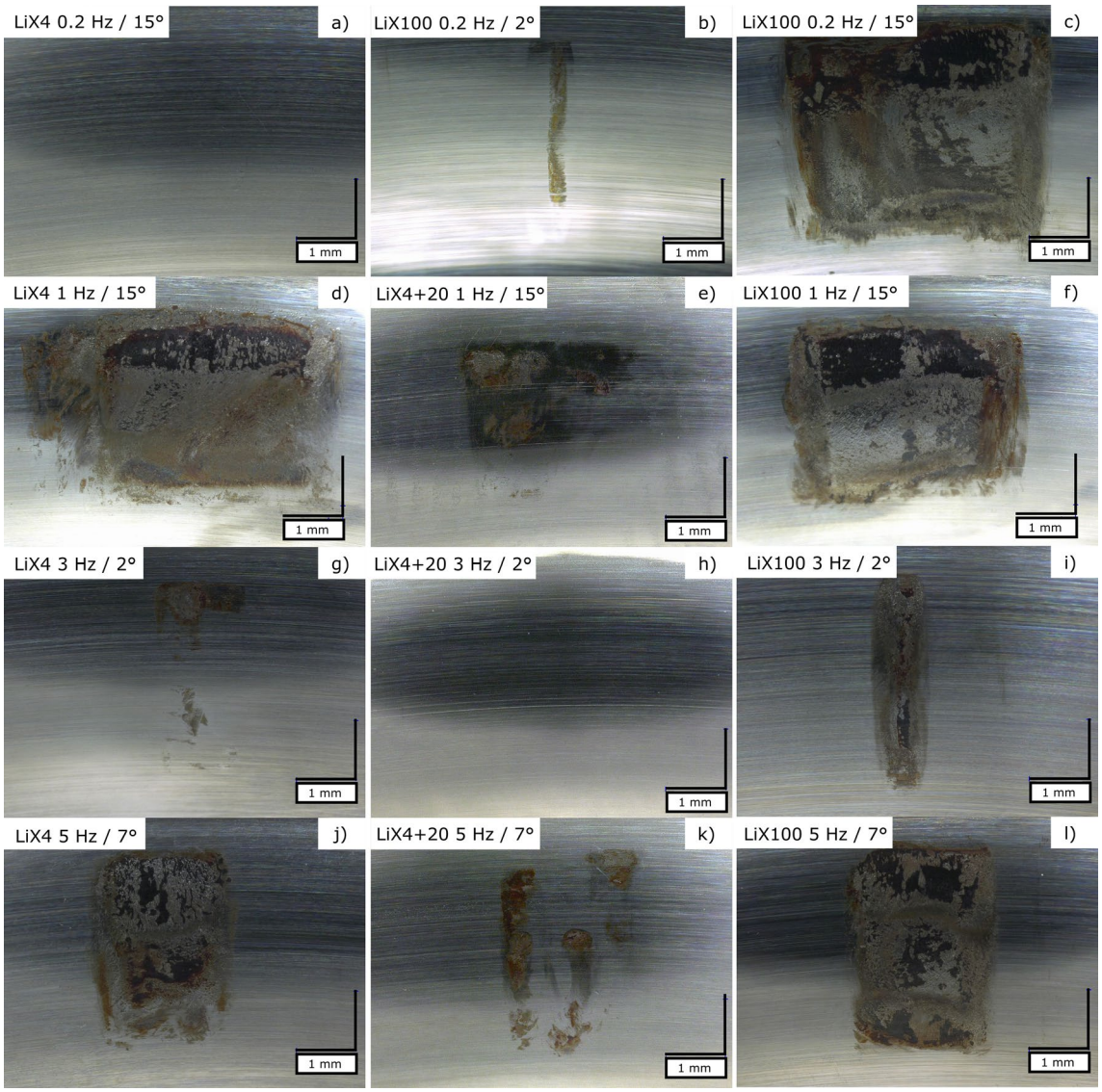

Fig. 4 Damage on the inner raceway of the bearing for different oscillation parameters and the corresponding grease. **a** Fresh surface, **b** f= 3 Hz, Θ= 15°, Grease 1, **c** f= 1 Hz, Θ= 2°, Grease 1, **d** f= 2 Hz, Θ= 15°, Grease 2. The parameter combinations on which the images are based are marked with the corresponding letter in Fig. 5

LiX100 grease at 3 Hz in Fig. 4i, it is the first condition under which the torque for the 2° test does not recover to the low initial level and a severely damaged raceway surface is the consequence. For the tests with LiX4+20, the increase in oscillation frequency also leads to an increase in torque for the tests at 15° and 30°. For the other oscillation angles, the curves have a similar shape when compared to the lower frequencies, even though the torque levels for the 15° test are a little lower.

At 5 Hz oscillation frequency, the torque for the tests with LiX4 at 7° and 15° reaches very high values of up to 18 Nm. At 2°, the curve has a similar shape to the one at 3 Hz but does not recover to its initial level any more. For the LiX4+20 grease, the test at 7° now shows an upward deflection for the first time. The shape of the curves for the other oscillation angles is similar to the ones at 3 Hz. Comparing the damage images in Fig. 4, line 4 at an oscillation frequency of 5 Hz and oscillation angle of 7°, it is clear that the surfaces for LiX4 and LiX100 are severely damaged on the whole track, whereas the surface is just partly damaged for the LiX4+20 grease with added base oil. For LiX100 and the test at 2°, the torque reaches higher levels than for the lower frequencies. The other curves behave similar to the other frequencies even though the torque at 15° is not rising as high during the early phase of the test.

Finally, for this part, there are two types of curves in the case of damage initiation: on the one hand, curves that

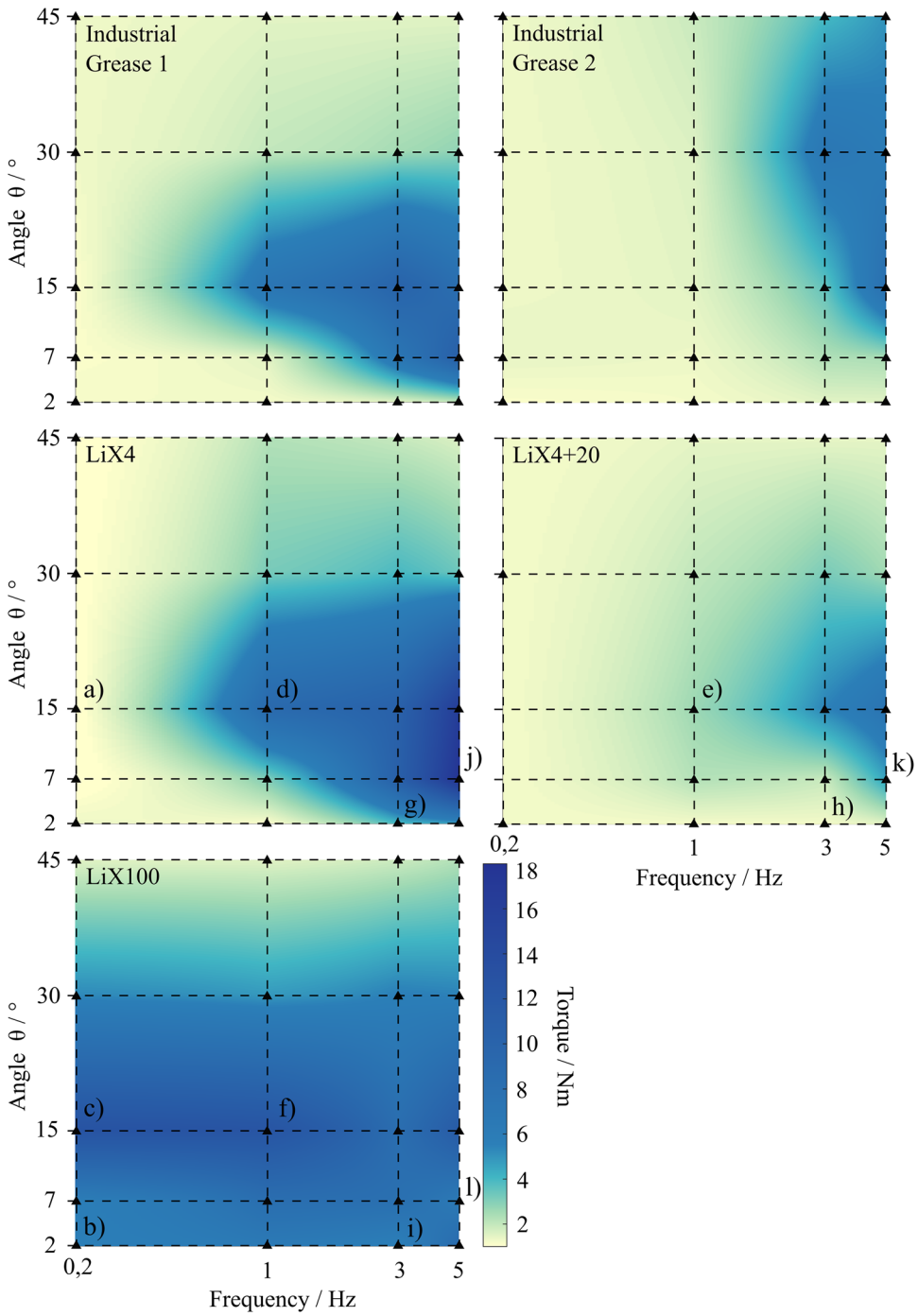

Fig. 5 Maximum friction torque reached during the corresponding test run. The examined parameter combinations are marked with black triangles. High torque values are represented by dark blue color. Values between the test parameters are interpolated linearly for visualization. The upper maps show the results for industrial grease 1&2 that were obtained in previous work [16]. The maps below show the corresponding results for the model greases investigated in this paper (Color figure online)

rise continuously until the end of the test period or remain at a constantly high level after the initial rise, and on the other hand, curves that reach a high torque peak and then drop to a low level. Regardless of the torque behavior, it can be said that reaching high torque values results in serious damage to the raceway surface. However, curves that approach a low torque level after damage initiation may turn out to be less critical in long-term tests. The following analysis focuses on the maximum torque values, regardless of the behavior of the torque curve.

3.2 Aggregation and Visualization of the Results

In order to get a more compact overview of the numerous results that have been compiled and to be able to link them

to a starvation model, a method was developed to display the results in such a way that a direct visual comparison is possible. The maximum torque reached during an experiment is assigned as characteristic torque value to each test run. This is illustrated in Fig. 2. In Fig. 5, each parameter combination is associated with its characteristic torque value and a corresponding color value. The tested parameter combinations are marked by black triangles. The torque values are linearly interpolated between the tested operating parameter combinations, resulting in a color map for each grease that ensures good clarity of the results. The color scale ranges from light yellow for low torques of 1 Nm to dark blue for high torque values of up to 18 Nm. Additionally, a qualitative assessment of the damage marks on the load side test bearing is made. This was achieved by means of a simple visual observation of every damage mark on the inner and outer raceway of the bearings. Each mark is rated either undamaged, partially damaged or fully damaged. Undamaged means that no corrosive or adhesive damage can be detected on the surface. In this case, the mark is represented by a light yellow box in the corresponding position on the bearing ring in Fig. 6. Partially damaged means that only parts of the track on the raceway that was covered by the rolling element during the oscillation shows corrosive or adhesive damage. These marks are represented by light green colored boxes. If the whole covered track is severely damaged, the mark is rated as fully damaged and represented by a dark blue box in Fig. 6. The installation position of the bearing with respect to the direction of gravity is also represented so that the influence of gravity on the position of the damage marks can be taken into account.

Figures 5 and 6 show the aggregated results of the three model greases that were tested in the course of this paper and additionally the results of two fully formulated industrially relevant greases that were tested in the previous paper [16]. Looking at Fig. 5a, distinct area for all the test greases is noticeable where high torque values can be observed. For most of the greases, this area is formed around medium oscillation angles and medium-to-high oscillation frequencies. An exception is the LiX100 grease that shows high torque values over the whole range of oscillation frequencies. In this results section, only the model greases will be investigated further. A detailed description of the results for the industrial greases can be found in [16]. For the following discussion in Sect. 4, however, the results are important.

Comparing the color maps for LiX4 and LiX4+20, it immediately becomes clear that the dark blue area becomes smaller. In general, the maximum torque values observed are lower and the dark blue area shifts toward higher oscillation frequencies. The maximum torque for the test at 1 Hz and 15° for LiX4 is 9.05 Nm where as it is at only 2.64 Nm for LiX4+20. Also, in the range of small oscillation angles, the damage area can be reduced by the grease with higher base oil content. Especially, the parameter combinations in the lower right corner at 3 Hz & 7°, 3 Hz & 2° and 5 Hz & 2° show a lower degree of damage when comparing the torque values and evaluating the damage marks. Comparing the results for oscillation angles of 30° and over, a slight improvement of the results for the grease with added base oil can be observed. However, the effect is not as strong, compared to smaller oscillation angles. In conclusion, additional base oil and a consequently increased oil separation rate lead to less damage and lower torque for all operating parameters.

To show the influence of base oil viscosity, we compare LiX100 and LiX4. A clear difference is that for LiX100, the damage area extends to low oscillation frequencies of 0.2 Hz. The test at 0.2 Hz and 15° interestingly shows the highest torque value out of all the tests with LiX100. The grease also shows worse results at small oscillation angles. The tests in the lower left corner of the maps show that there was almost no increase in torque and only a few partly damaged marks for LiX4 and the tests at 2° & 0.2 Hz/ 1 Hz, whereas for LiX100, significantly higher torque values paired with more damaged marks were the result. It must be noted that the high torque values and thus also the surface damage in this range for LiX100 were observed at the beginning of the experiments, see Fig. 3. In the course of the experiments, the torque decreased again. Looking at an angle of 30°, we can see that the damage area is spread to lower frequencies. The results for 30° and frequencies of 1 Hz, 3 Hz and 5 Hz are comparable to those of LiX4 with slightly more damage. At 45° oscillation angle, the bearings with LiX100 as well as with LiX4 show less damage compared to smaller oscillation angles.

3.3 Connection of Experimental Results and Proposed Starvation Number

In our previous paper, we proposed the starvation number shown in Equation 1, which takes into account lubricant parameters and operating conditions of the oscillating rolling element bearing.

$$SN = \frac{\eta_0 \cdot a \cdot f_c}{\sigma_s \cdot O_{SR}} \cdot \begin{cases} \frac{x}{2b} & \text{if } x \le x_{SW} \\ \frac{x_{SW}}{2b} \cdot \frac{x_c - x}{x_c - x_{SW}} & \text{if } x_c \ge x > x_{SW} \\ 0 & \text{if } x > x_c \end{cases} \quad (1)$$

The values of the operating parameters that are necessary for the calculation of the starvation number are listed in Table 2. This includes the rollover frequency f_c which is twice the oscillation frequency f, the length of the long HERTZ'ian half axis a over which the rolling element load is taken into account, and the distance x which describes the path covered by the rolling element on the raceway. By division with

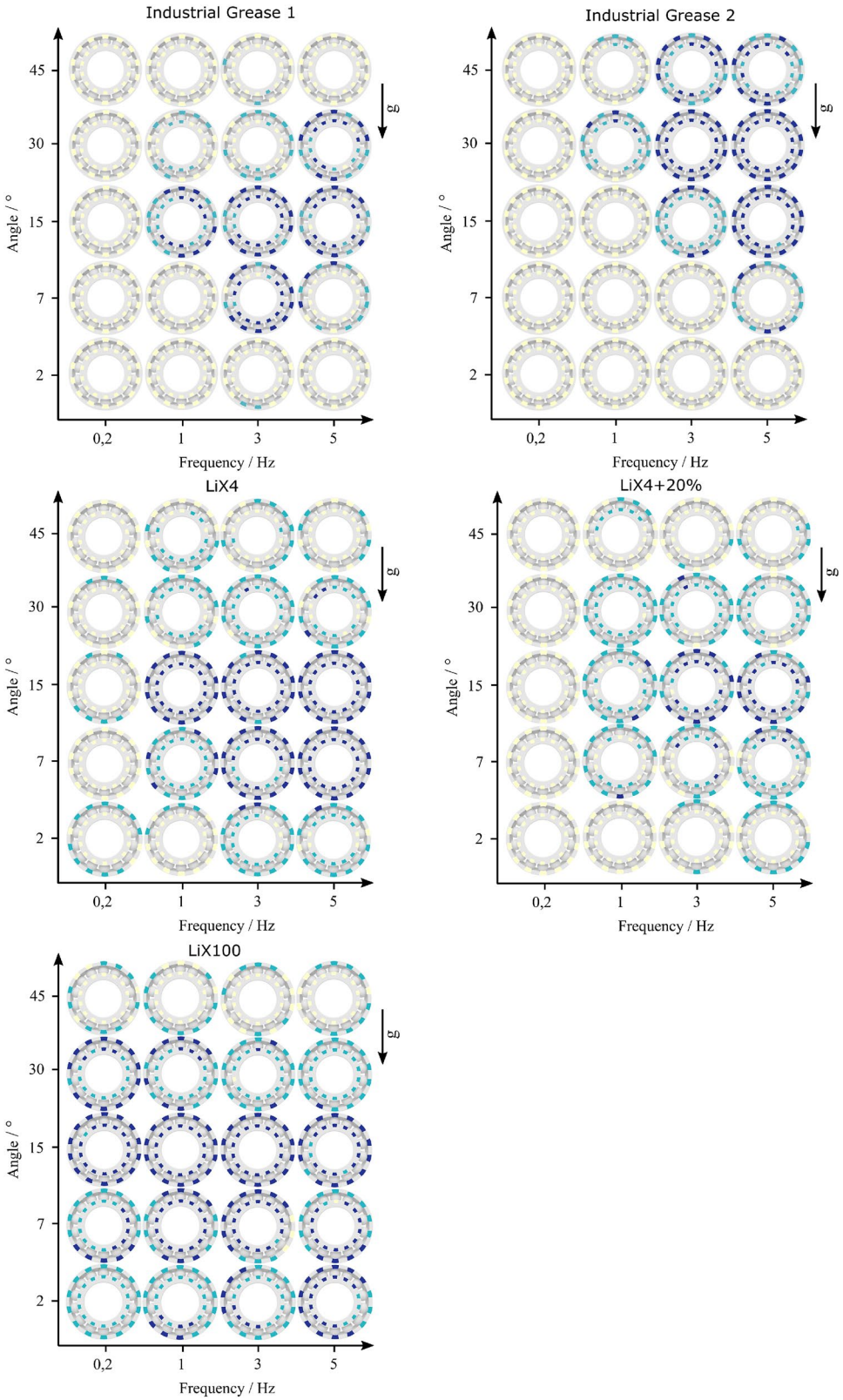

Fig. 6 Overview over the damaged areas on the bearing raceway surface on the outer and inner ring. Areas that are completely damaged are marked in dark blue; areas that are partly damaged are marked in turquoise; areas without severe damage are marked in light yellow. The upper maps show the results for industrial grease 1&2 that were obtained in previous work [16]. The maps below show the corresponding results for the model greases investigated in this paper (Color figure online)

the short HERTZ'ian half-axis x is made dimensionless. The distance x_{sw} is the distance at which the wear-critical area spreads out most toward low frequencies. The critical distance x_c is the distance at which the operating conditions become uncritical over the entire frequency band. The necessary grease parameters can be found in Table 1. This

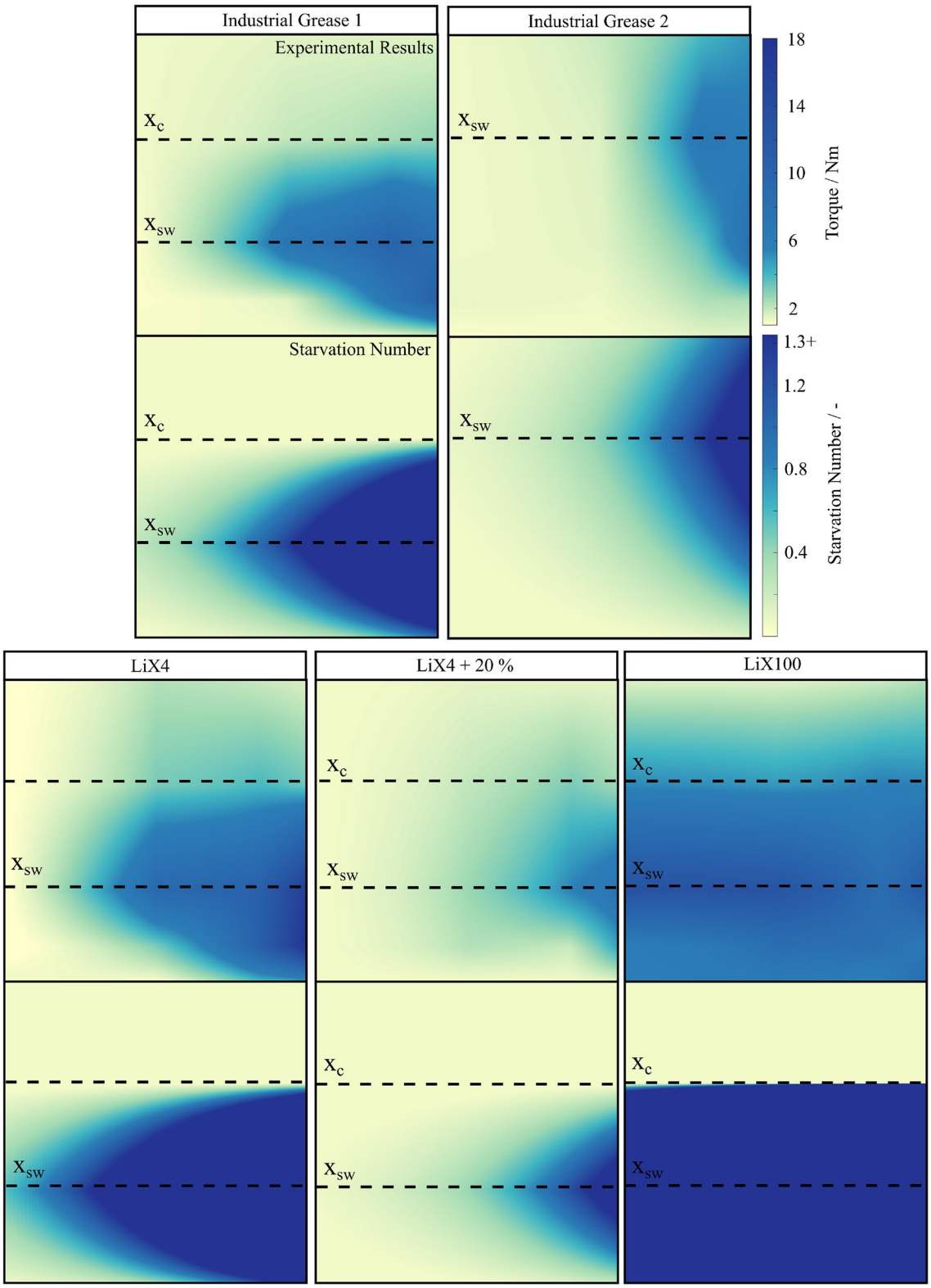

Fig. 7 Comparison of the experimental results with the calculated starvation number on the inner ring contact. For each grease, the upper map shows the experimental results and the lower map the calculated Starvation Number S_N. The maps in the upper half of the figure show the results for industrial grease 1&2 that were obtained in previous work [16]. The maps below show the corresponding results for the model greases investigated in this paper

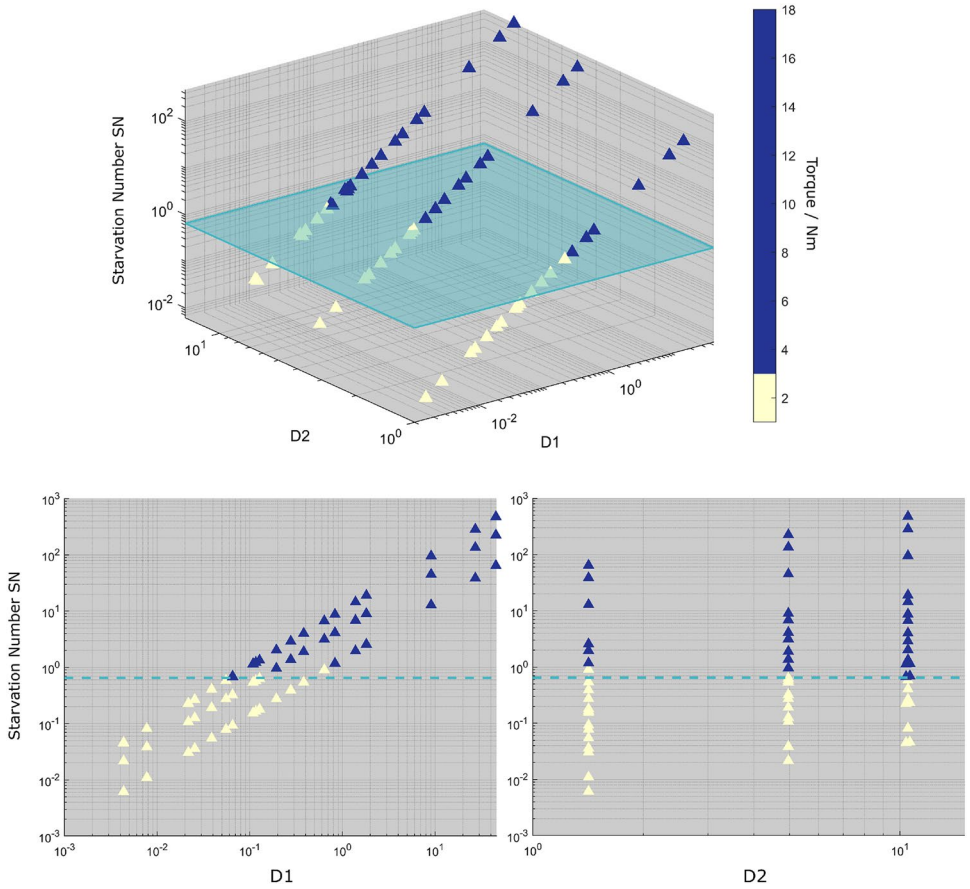

Fig. 8 Summary of all results based on the dimensionless Starvation Number SN and the torque values. The Starvation Number of the tests is represented over its two dimensionless components D1 and D2. Each test is represented by a triangle that is colored according to the maximum torque value reached during the test (Color figure online)

includes the dynamic base oil viscosity η_0, the oil separation rate O_{SR} as well as the surface tension of the base oil σ_s. The starvation number *SN* is calculated in the range of the tested operating parameters and each corresponding grease. To provide a visual representation of the starvation number, the values are assigned to colors similar to the color maps that represent the characteristic torque values. Figure 7 shows a comparison of the torque values in the experiments and the corresponding starvation number. In the top left of Fig. 7, you can see the color maps for industrial grease 1, that was investigated in previous work. The upper color map shows the experimental torque result with the determined distances x_{sw} and x_c, the underlying map displays the corresponding starvation number S_N. The upper right shows the results for industrial grease 2, which was investigated in previous work. The diagrams in the bottom row show the test results with the model greases, starting left with LiX4, LiX4+20 in the middle, and LiX100 on the right.

Comparing the torque maps of the LiX4 and the LiX4+20, we observed that the critical damage area becomes smaller and moves to higher frequencies. If we compare the starvation number of the two greases, we see similar behavior. The increase in base oil content for the LiX4+20 grease leads to an increase in oil separation (O_{SR}) of 4.2 % as shown in Table 1. The oil separation is the only parameter that differs in the starvation number of the two greases. The torque maps of the LiX4 and the LiX100 show that the damaged area spreads over the whole parameter range except for an oscillation angle of 45°. The starvation number of two greases differs mainly due to the significantly increased (factor 56) base oil viscosity. This means that the starvation number in the investigated parameter range increases significantly up to the defined critical angle θ_c and the corresponding distance x_c. The visualization by means of the color maps shows that the starvation number can describe the tendency of the test results qualitatively.

To give an overview over the achieved results, all test result are presented in a summary diagram in Fig. 8. The two dimensionless parts of the Starvation Number D1 (2) & D2 (3) are plotted on the logarithmic *x* and *y* axes.

$$D_1 = \frac{\eta_0 \cdot a \cdot f_c}{\sigma_s \cdot O_{SR}} \tag{2}$$

$$D_2 = \begin{cases} \frac{x}{2b} & \text{if } x \le x_{\mathrm{SW}} \\ \frac{x_{\mathrm{SW}}}{2b} \cdot \frac{x_{\mathrm{c}} - x}{x_{\mathrm{c}} - x_{\mathrm{SW}}} & \text{if } x_{\mathrm{c}} \ge x > x_{\mathrm{SW}} \\ 0 & \text{if } x > x_{\mathrm{c}} \end{cases} \quad (3)$$

The Starvation Number, which is a product of two dimensionless parts, is shown on the z-axis. The Starvation Number for each test is marked as a triangle in the spanned space. The triangles are colored in a binary color code based on the maximum torque value that was reached during the test. If the maximum torque exceeded a threshold of 3 Nm, the triangle is colored dark blue, otherwise light yellow. The green plane marked in the diagrams indicates the critical Starvation Number $S_{Nc} = 0.65$ under which no test exceeded the threshold value of 3 Nm. Above this number, most of the tests show very high torque values and severely damaged raceways.

4 Discussion

The starvation number S_N is based on the assumption, that after a certain number of cycles, re-lubrication of the contact at small oscillation angles takes place mainly due to bled base oil [6]. A high starvation number indicates that under these conditions, the contact cannot be sufficiently supplied with base oil, i.e., severe starvation occurs and no sufficiently separating lubricating film can be formed in the contact. This results in boundary lubrication and damage initiation. The results show that an increase in the base oil content and an associated increase in oil separation lead to a reduction in the damage-critical parameter range. These results thus support the hypothesis underlying the Starvation Number. It should be noted, however, that increasing the base oil content not only increases the oil separation but also decreases the consistency, as shown in Table 1. Therefore, it cannot be excluded that the consistency also has a considerable influence on the grease performance. Assuming that the reflow of the base oil is responsible for supplying the contact, the viscosity and the associated mobility of the base oil also play a crucial role. A low-viscosity oil can flood the track behind the rolling element faster than a high-viscosity base oil [18]. To test this hypothesis, the model grease LiX4 with a low-viscosity base oil was compared with the model grease LiX100 with a high-viscosity base oil. In Table 1, we can see that both model greases have the same consistency and comparable oil separation rates O_{SR}. Nevertheless, the damage-critical parameter range for LiX100 is significantly extended, especially toward low oscillation frequencies and small oscillation angles. In this case, the increased base oil viscosity η_0 thus seems to have a decisive influence on starvation in the contact zone. This fact supports the consideration of the base oil viscosity in the denominator of the starvation number. At this point, however, it must be emphasized once again that for the evaluation of the test results in the color maps, the maximum torque during the experiments was used. For the tests with industrial grease 1, industrial grease 2 and the model greases LiX4 and LiX4+20, these values generally also match the torque values at the end of the test run. However, some of the torque curves of the tests with LiX100 behave differently. In some cases, an increase in torque and the associated initiation of damage can be observed at the beginning of the test, followed by a steady drop in torque to relatively low torque values.

It is therefore possible that these operating parameters would not be as critical for long-term operation as they appear from this observation.

The influence of the oil separation rate (O_{SR}) and base oil viscosity on the development of damage-critical parameter combinations, especially in the area of small angles, could be plausibly explained on the basis of the experimental results. Up to now, x_{sw} and x_{c} have to be obtained empirically from test data. In order to develop a starvation number that can be used solely based on bearing geometry and grease parameters, a physical relationship between critical angle and geometry must be found. The reason that larger oscillation angles are less critical with regard to starvation is assumed to be a geometric relationship. From a sufficiently large oscillation angle onward, the contact track may be replenished by grease reservoirs from the cage. Also, due to the cage contact, piled up grease dams on the sides of the track could be smoothed and thus lead to a re-lubrication of the track. A similar replenishment mechanism was already mentioned by [24] for rotating grease-lubricated bearings. For the lithium greases, significantly less critical operating parameters are observed from an oscillation angle of 30°. However, we can see that the grease parameters also have a decisive influence on the critical angle. Industrial grease 2, which is a calcium grease and thus has a significantly different thickener structure to the other greases, shows a larger starvation driven wear angle θ_{sw} as well as a larger critical angle θ_{c}. From these observations, we deduce that other grease parameters also have a decisive influence in the region of larger oscillation angles. Another point to be discussed is the influence of grease additives on wear initiation. The results have shown that critical parameter combinations will lead to an early wear initiation with the model greases that do not contain additives but also with the fully formulated industrial greases. The results indicate that the additives do not have a significant effect under the tested conditions. To obtain a more tangible result, we added a common anti-wear friction modifier package containing ZDDP and MoDTC additives to the LiX4 model grease in order to be able to directly observe the influence of the

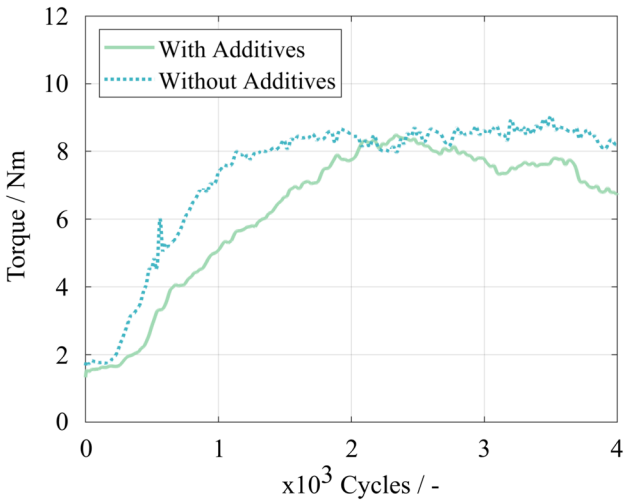

Fig. 9 Comparison of a test at 1 Hz and 15° with LiX4 grease without additives and LiX4 with added 2 % liquid and 2 % solid additives

additives in the test. The results are shown in Fig. 9. Comparing the dotted dark green torque curve for the test without additives and the solid light green torque curve for the grease with additives, we see that for both of the experiments, the torque starts rising after just a few hundred oscillation cycles up to a value of over 8 Nm. With the experience from the other wear tests, it can be said that there is no qualitative difference in terms of wear initiation and the influence of the additives in this critical parameter range is negligible. It must be said that this direct comparison of the model grease with and without additives was only carried out for a very critical parameter combination, in which severe starvation, boundary lubrication and damage initiation with a strong torque increase occurred after a short time. Under less critical operating parameter combinations, additives could have a wear-reducing effect in longer test runs. At this stage, the purpose of the surface tension σ_s is to make the Starvation Number S_N dimensionless since the surface tension hardly differs between the base oils used. However, from a physical point of view, we expect the surface tension to have a significant impact.

5 Conclusion and Outlook

In previous work, we have shown that oscillating motion in highly loaded grease-lubricated rolling element bearings can cause severe damage to the bearing raceway after only a few oscillating cycles. On this basis, a Starvation Number S_N was proposed which, taking into account the grease and operating parameters, predicts a tendency of the conditions to cause early wear initiation. Decisive grease parameters in the Starvation Number are the oil separation rate O_{SR} and the base oil viscosity η_0. In order to investigate the influence of these parameters, additive-free lithium complex greases were produced, which differ mainly in the base oil viscosity and the oil separation rate. With these model greases, it was shown that an increased oil separation reduces the range of damage-critical operating parameters and reduces the severity of occurring damage. However, an influence of the grease consistency cannot yet be fully ruled out on the basis of these tests. The comparison of two model greases with very different base oil viscosities showed that a high base oil viscosity performs significantly worse at low oscillation frequencies and small oscillation angles than a grease with a lower base oil viscosity. The experiments with the model greases show that the starvation number is a good indicator whether the operating conditions are critical for wear initiation or not, at least with respect to the studied grease parameters. The influence of additives seems to be negligible in the investigated parameter range. Based on the results obtained, a grease with a high oil separation rate and low base oil viscosity is recommended for use in grease lubricated, highly loaded oscillating rolling element bearings. In addition, based on the results to date, it is recommended that a critical Starvation Number S_{Nc} of 0.65 should not be exceeded. The aim of future research is to make the determination of the starvation-driven wear angle θ_{sw} and the critical angle θ_c independent of empirical investigations and to determine these parameters entirely from the lubricant and geometry parameters of the bearing. The influence of the bearing cage will for this purpose be a major focus. It will also be necessary to investigate how the Starvation Number S_N can withstand scaling to other bearing sizes and other bearing geometries.

Acknowledgements The authors would like to thank Muyuan Liu, Josephine Kelley, and Volker Schneider for their professional advice, Marvin Woersdoerfer for the help with the experimental work and Peter Schönemeier for the help with the commissioning of the test rig. This document is a result of the research project HBDV 'Highly Accelerated Pitch Bearings' (Grant number 0324303A) funded by the Federal Ministry for Economic Affairs and Climate Action (Germany).

Author Contributions All authors contributed to the study conception and design. Material preparation, data collection and analysis were performed by SW, BL, JG, JL. The first draft of the manuscript was written by SW, NB and JL. FS and GP commented on previous versions of the manuscript. GP was responsible for the funding acquisition. All authors read and approved the final manuscript.

Funding Open Access funding enabled and organized by Projekt DEAL. This document is a result of the research project HBDV 'Highly Accelerated Pitch Bearings' (Grant number 0324303A) funded by the Federal Ministry for Economic Affairs and Climate Action (Germany).

Declarations

Competing interest The authors have no relevant financial or non-financial interests to disclose.

References

1. Burton, T., Sharpe, D., Jenkins, N., Bossanyi, E.: Wind Energy Handbook, 2nd edn. Wiley & Sons, London (2012)
2. Stammler, M., Thomas, P., Reuter, A., Schwack, F., Poll, G.: Effect of load reduction mechanisms on loads and blade bearing movements of wind turbines. Wind Energy **23**, 274–290 (2020)
3. Grebe, M., Molter, J., Schwack, F., Poll, G.: Damage mechanisms in pivoting rolling bearings and their differentiation and simulation. Bear. World J. **3**, 71–86 (2018)
4. Schwack, F., Bader, N., Leckner, J., Demaille, C., Poll, G.: A study of grease lubricants under wind turbine pitch bearing conditions. Wear **454–455**, 203335 (2020)
5. Grebe, M.: False brinelling—standstill marks at roller bearings. Dissertation, Slovak University of Technology, Bratislava (2012)
6. Cann, P.M.E., Chevalier, P., Lubrecht, A.A.: Track depletion and replenishment in a grease lubricated point contact: a quantitative analysis. Tribol. Ser. **32**, 405–413 (1997)
7. Cann, P., Spikes, H.: Visualisation of starved grease and fluid lubricant films. Tribol. Ser. **30**, 161–166 (1995)
8. Cann, P.: Starvation and reflow in a grease-lubricated elastohydrodynamic contact. Tribol. Trans. **39**(3), 698–704 (1996)
9. Cann, P.: Starved grease lubrication of rolling contacts. Tribol. Trans. **42**(4), 867–873 (1999)
10. Astrom, H., Ostensen, J.O., Hoglund, E.: Lubricating grease replenishment in an elastohydrodynamic point contact. J. Tribol. **115**(3), 501–506 (1993)
11. Lugt, P.M.: A review on grease lubrication in rolling bearings. Tribol. Trans. **52**(4), 470–480 (2009)
12. Lugt, P.M.: Grease Lubrication in Rolling Bearings. Wiley, New Jersey (2012)
13. Kita, T., Yamamoto, Y.: Fretting wear performance of lithium 12-hydroxystearate greases for thrust ball bearing in reciprocating motion. J. Jpn. Soc. Tribol. **42**(6), 492–499 (1997)
14. Shima, M., Jibiki, T.: Fretting wear. J. Jpn. Soc. Tribol. **53**(7), 462–468 (2008)
15. Maruyama, T., Saitoh, T.: Oil film behavior under minute vibrating conditions in EHL point contacts. Tribol. Int. **43**(8), 1279–1286 (2010). https://doi.org/10.1016/j.triboint.2009.11.004
16. Wandel, S., Bader, N., Schwack, F., Glodowski, J., Lehnhardt, B.: Starvation and relubrication mechanisms in grease lubricated oscillating bearings. Tribol. Int. **165**, 107276 (2022)
17. Harris, T., Kotzalas, M.: Rolling Bearing Analysis: Essential Concepts of Bearing Technology. CRC Press, Boca Raton (2007)
18. Damiens, B., Lubrecht, A., Cann, P.: Lubrication regimes in rolling element bearings. Tribol. Ser. **39**, 295–301 (2001)
19. Cann, P., Damiens, B., Lubrecht, A.: The transition between fully flooded and starved regimes in EHL. Tribol. Int. **37**(10), 859–864 (2004)
20. Cen, H., Lugt, P.M.: Replenishment of the EHL contacts in a grease lubricated ball bearing. Tribol. Int. **146**, 106064 (2020)
21. Schwack, F., Prigge, F., Poll, G.: Finite element simulation and experimental analysis of false brinelling and fretting corrosion. Tribol. Int. **126**, 352–362 (2018). https://doi.org/10.1016/j.triboint.2018.05.013
22. Harris, T., Rumbarger, J., Butterfield, C.: Wind turbine design guideline DG03: Yaw and pitch rolling bearing life. Technical report, NREL (2009). https://doi.org/10.2172/969722
23. Schwack, F., Schneider, V., Wandel, S., de la Presilla, R.J., Poll, G., Glavatskih, S.: On the critical amplitude in oscillating rolling element bearings. Tribol. Int. 107154 (2021)
24. Damiens, B., Lubrecht, A., Cann, P.: Influence of cage clearance on bearing lubrication. Tribol. Trans. **47**(1), 2–6 (2004)